Conference Proceedings
Solar World Congress 2015
Daegu, Korea, 08 – 12 November 2015

Zirconium carbide-nitride composite matrix based solar absorber structures on glass and aluminum substrates for solar thermal applications

[a]Belal Usmani, [b]Vivek Vijay, [c]Rahul Chhibber, [c]Laltu Chandra [a]Ambesh Dixit*

[a] Department of Physics, Indian Institute of Technology Jodhpur, Rajasthan, 342011, India
[b] Department of Mathematics, Indian Institute of Technology Jodhpur, Rajasthan, 342011, India
[c] Department of Mechanical Engineering, Indian Institute of Technology Jodhpur, Rajasthan, 342011, India

Abstract

Zirconium carbide-nitride absorber (ZrC-ZrN) and zirconium reflector tandem structures were prepared on glass and aluminum substrate, in conjunction with zirconium oxide (ZrO_x) anti-reflection coatings, using DC/RF magnetron sputtering system. The solar absorption properties of zirconium carbide-nitride absorber layers were optimized by controlling nitrogen flow during synthesis process for optimal solar thermal response. X-ray diffraction (XRD), scanning electron microscopy (SEM) and atomic force microscopy (AFM) measurements were carried out on fabricated absorber-reflector tandem structures to understand the structure-property correlation. We absorbed strong dependence of zirconium nitride fraction on solar thermal performance. We observed enhanced solar absorptance $\alpha \sim 0.86$ and thermal emittance $\varepsilon \sim 0.05$ at room temperature for structures fabricated with optimized synthesis parameters. The optimized structures are stable up to 150 °C in the air without any significant degradation in their solar performance.

Keyword: *Solar selective coatings, Sputtering, Structure, Optical property, Thermal stability*

1. Introduction

Solar thermal energy is getting attention due to its potential as compared to the other renewable energy resources. This can be used in various forms such as low temperature applications, e.g. solar water heating applications, intermediate and high temperature applications e.g. process heating (Mekhilef et al., 2011), power applications (Selvakumar and Barshilia, 2012). Such systems usually consist of several sub-systems such as collection/concentration of light, absorption/conversion of light into thermal energy and utilization to convert into electrical energy or for other application. The light to thermal energy conversion subsystem consists of special collection tubes, called as solar collectors (Kalogirou, 2004; Selvakumar and Barshilia, 2012). These collectors are coated with spectrally selective coatings, having a high absorptance in the wavelength range of 0.3- 2.5 μm and low emittance in wavelength range 2.5 to 25 μm in the mid to higher operating temperature ranges (Seraphin, 1997). The development of thermally stable solar selective coating is important for the maintenance free continuous operation of solar thermal systems/subsystems. There are continuous efforts to develop such material systems, which can withstand temperature, environmental conditions, and large thermal cycling for efficient photothermal conversion. Numerous solar selective coatings are developed using physical vapor deposition for mid-temperature (100 °C < T < 400 °C) applications. Some of them are commercialized successfully. For example, Zhang et al. developed SS-Al coatings using DC magnetron sputtering, with absorptance in the range of 0.93 - 0.96 and emittance of ~ 0.03 - 0.04 at room temperature. These are thermally stable upto 1h at 500 °C in vacuum (Zhang et al., 1998a, 1998b) and are used on evacuated glass tubes for solar hot water and steam applications. Lazarov's group

doi:10.18086/swc.2015.04.02 Available at http://proceedings.ises.org

developed TiN_xO_y oxynitride coatings with SiO_2 antireflection coatings on Cu and Al substrates with α=0.94 and ε=0.04 at 100 °C (Lazarov, 1993). S-Solar, Sweden, developed Ni-NiO metal-dielectric composite based absorber coating on Al substrates, with absorptance in the range 0.94-0.96 and thermal emittance of 0.13-0.15 at 100 °C for low temperature applications (Wackelgard and Hultmark, 1998). Electrodeposited black Chrome ($Cr-Cr_2O_3$) cermet coatings on Ni, Fe, Cu, stainless-steel substrate are developed and commercialized by by MTI in the United State and several other research and development groups (Bogaerts and Lampert, 1983; McDonald, 1975; Driver, 1981; Ignatiev et al., 1979; Smith et al., 1984; Sweet et al., 1984; Lampert, 1980; Holloway et al., 1980). H.C. Barshilia et al. developed $Cr_xO_y/Cr/Cr_2O_3$ transition metal oxide based multilayer absorber on Cu substrates for mid-temperature applications, exhibiting high absorptance (0.89-0.91) and low emittance at 82 °C (0.05-0.06) (Barshilia et al., 2008). N. Selvakumar et al and Vannoni et al have developed CrMoN/CrON tandem absorber on SS substrate with high absorptance (0.90 - 0.92) and low thermal emittance (0.13 - 0.15) for mid-temperature applications (Selvakumar et al., 2013, Vannoni et al., 2008). Yet such systems exhibit poor performance at elevated temperatures, especially thermal emittance at elevated temperatures, causing thermal loss in solar thermal systems. The oxidation of the metal content is the main reason for degradation of optical and thermal response in these cermet structures (Barshilia et al., 2008; Sebastian et al., 1997). Alike such oxide cermet structures, refractory metal carbo-nitride absorber systems may show significant improvement in their thermal stability in conjunction with their solar thermal performance. Considering the same, we investigated the solar thermal performance of zirconium carbide-nitride absorber- zirconium reflector tandem structures with zirconium oxide antireflection coating layer on glass and aluminum substrates.

2. Experimental details

The zirconium carbo-nitride absorber- zirconium reflector tandem structures were deposited on glass and aluminum substrate using DC/RF reactive magnetron sputtering. High purity (99.8%) zirconium (Zr) metal and (99.9%) ZrC targets were integrated with 4'' magnetron sputter gun for depositing Zr metal reflector, zirconium carbo-nitride absorber and zirconium oxide antireflecting coatings on glass and aluminum (Al) substrates. The glass substrates (25 x 76 x1 mm^3) were ultrasonically cleaned for 5 min in acetone and ethanol baths, respectively, without any mechanical polishing. Aluminum substrates were first mechanically polished with 2000 grade SiC abrasive paper to remove oxide layer and to reduce surface roughness, followed by ultrasonic cleaning in isopropyl alcohol and acetone for 10 minutes respectively. These cleaned substrates were used for fabricating the solar selective coating structures. The base pressure of deposition chamber was brought down ~ 6.0 x 10^{-6} mbar and sputtering processes were carried out at a constant working pressure ~ 2.0 x 10^{-2} mbar. The targets were pre-sputtered for ~15min before deposition of respective layers to clean any surface impurities such as oxide layers and process impurities. The detailed experimental process for deposition of individual layers is explained elsewhere (Usmani et al., 2015). Crystal phases and structure, microstructure and surface properties and elemental composition of the synthesized zirconium carbo-nitride absorber- zirconium reflector tandem structures in conjunction with zirconium oxide antireflection films were measured using X-ray diffraction (XRD), scanning electron microscope (SEM), atomic force microscope and X-ray energy dispersive system measurements. The reflectance spectra were measured in wavelength range (0.3 to 2.5 μm) by using Carry 5000 UV-Vis-NIR spectrophotometer in conjunction with standard Spectralon reference. The absorptance α was calculated using these measured reflectance spectra with respect to AM 1.5 solar spectrum. FTIR reflectance measurements were carried out in wavelength range (2.5 to 25 μm) and used to calculate the room temperature thermal emittance, ε. The thermal stability of these structures was studies by heating samples at ~ 150 °C for 2 hours at a constant heating rate ~ 5 °C/min, followed by free cooling to the room temperature. Thermal impact was investigated characterizing the structural/microstructural changes to understand the structure-property correlation on solar thermal performance on these zirconium carbo-nitride absorber-reflector structures.

3. Results and discussions

3.1 X-ray diffraction analysis

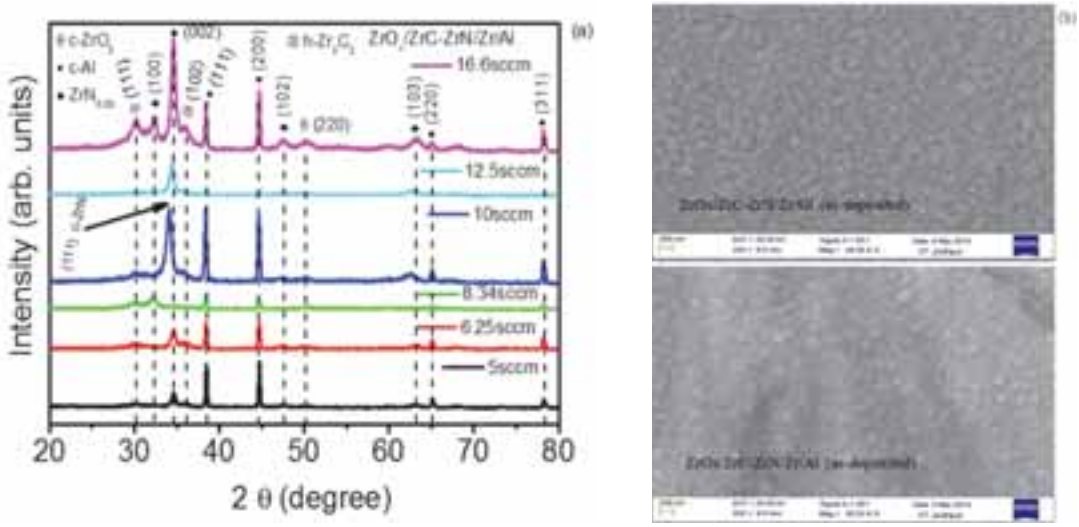

Fig. 1: (a) XRD spectra of ZrO_x/ZrC-ZrN/Zr absorber-reflector tandem selective coatings on aluminum substrate for different N_2 flow rates used for ZrC-ZrN absorber layer. **(b)** SEM images of ZrO_x/ZrC-ZrN/Zr absorber-reflector tandem structure deposited on aluminum and glass substrates.

The XRD pattern of ZrO_x/ZrC-ZrN/Zr absorber-reflector tandem selective coatings coated on Al substrate are shown in Fig. 1(a), with varying nitrogen flow rates used for synthesizing these structures. The diffraction peaks at 2θ = 38.42°, 44.74°, 65.07° and 78.22° correspond to (111), (200), (220) and (311) reflection plane from the aluminum substrate in all these XRD graphs. A strong peak at 2θ = 34.57° and weak peaks at 2θ = 32.39°, 47.57° and 63.18° correspond (002) and (100), (102), (103) diffraction planes for hexagonal zirconium nitride (h-$ZrN_{0.28}$) phase, respectively. Whereas, weak diffraction peak at 2θ = 36.09° correspond to (102) hexagonal zirconium carbide (h-Zr_3C_2) phase. The measured volume fraction of zirconium nitride is much larger than that of zirconium carbide suggesting a carbide system in nitride matrix. XRD results, for absorber-reflector tandem structure on glass substrates, are similar to that on aluminum substrates except Al substrate XRD pattern. XRD results on glass substrates, also substantiate larger zirconium nitride volume fraction in fabricated structures. Anti-reflecting ZrO_x layer exhibit mixed phase with dominating tetragonal zirconium oxide phase, as indexed in Fig. 1(a) (top panel). ZrO_x top layer scanning electron micrographs are shown in Fig. 1(b) for as deposited absorber-reflector tandem structures on glass and aluminum substrates. As deposited surfaces are smooth for both aluminum and glass substrates with micro granular structures ~ 100 nm, as shown in Fig. 1(b). In contrast to glass substrates, the surface structure of absorber-reflector tandem structures on Al substrates consists of substrate imprints and average surface roughness is ~ 10 ± 2 nm for both substrates.

3.2 Optical properties

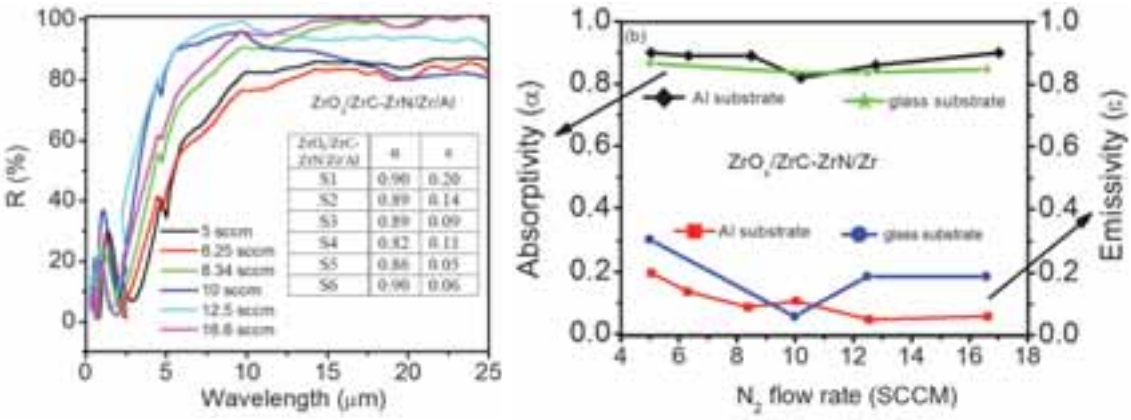

Fig. 2: (a) Reflectance spectra of absorber-reflector tandem selective coating deposited on aluminum substrate with varying nitrogen flow rate. **(b)** Calculated absorptance (α) and emittance (ε) values of absorber-reflector tandem structure selective coatings deposited on almunium and glass substrate.

The measured reflectance, as a function of wavelength, is plotted in Fig. 2(a) for ZrO_x/ZrC-ZrN/Zr absorber-reflector tandem structures on aluminum substrates in 0.2 – 25 μm range for different N_2 flow rates, used during synthesis. These reflectance measurments are used to calculate the absorptivity 'α' in ~ 0.3 – 2.5 μm range, and emissivity 'ε' in ~ 2.5 – 25 μm range, using Eq. (1) and (2);

$$\alpha = \frac{\int_{0.3}^{2.5} (1-R(\lambda)) I_{sun}(\lambda) d\lambda}{\int_{0.3}^{2.5} I_{sun}(\lambda) d\lambda} \quad (1)$$

$$\varepsilon = \frac{\int_{2.5}^{25} (1-R(\lambda)) E_b(\lambda) d\lambda}{\int_{2.5}^{25} E_b(\lambda) d\lambda} \quad (2)$$

Where $I_{sun}(\lambda)$ is ASTM G173-03 solar reference spectrum, AM1.5 and $E_b(\lambda)$ is the spectral radiance of a black body at temperature, T, and is given by Plank's law Eq. 3 (Duffie and Beckman, 1991) and R is the measured reflectance as a function wavelength. Here, Eq. 2 describes the emissivity against the total black-body radiation at given temperature T, which is defined as

$$E_b = \frac{C_1}{\lambda^5 [e^{C_2/\lambda T} - 1]} \quad (3)$$

Where $C_1 = 3.743 \times 10^{-16}$ W m^2 and $C_2 = 1.4387 \times 10^{-2}$ mK.

The measured values of α and ε are plotted in Fig. 2(b) as a function of different N_2 flow rates for both aluminum and glass substrates. The values of α and ε range from 0.86 – 0.90 and 0.05 – 0.14, respectively. The volumetric fraction of zirconium nitride strongly depends on the N_2 flow rates, and intermediate N_2 flow

rates produced optimal ZrN in ZrC-ZrN matrix structures. The absorber structure with maximum ZrN fraction showed optimal performance with absorptance ~ 0.86 and emittance ~ 0.05 for both substrates.

3.3 Thermal stability in air

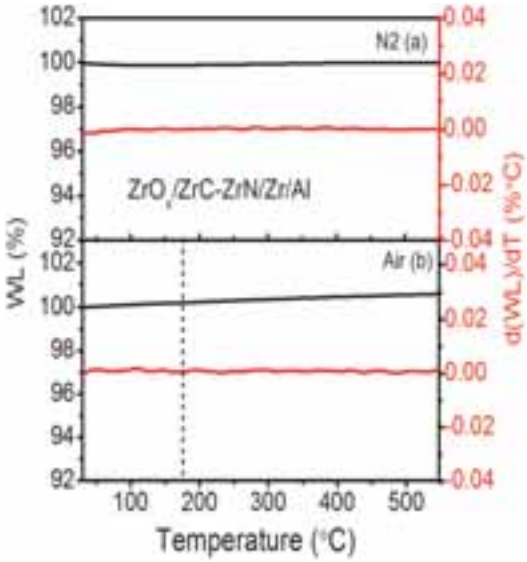

Fig. 3: Weight change percentage (WC %) versus temperature (°C) and differential of the weight change with temperature of ZrO_x/ZrC-ZrN/Zr absorber-reflector tandem selective structure deposited on aluminum substrate in (a) N_2 (b) air environment.

The ZrO_x/ZrC-ZrN/Zr absorber-reflector tandem selective structures were subjected to simultaneous thermal analysis (STA) measurements. The samples were heated upto 550 °C at a heating rate of 5 °C/min in nitrogen and air ambience. The measured weight change (WC) and differential weight change (d(WC)/dT) versus temperature are plotted in Fig. 3 for the best ZrO_x/ZrC-ZrN/Zr/Al sample with $\alpha \sim 0.86$ and $\varepsilon \sim 0.05$. These measurements did not exhibit any weight change under nitrogen ambience, whereas in air, weight gain started ~ 200 °C, as marked by dotted line in Fig. 3 (b). This weight gain was mainly due to oxidation of fabricated structures in air ambience, which was not observed in case of nitrogen ambience. These ZrO_x/ZrC-ZrN/Zr structures should be stable even at much higher temperatures, as Zr is the refractory material and ZrO_x top layer should avoid direct oxidation of underneath ZrC-ZrN absorber layer. Thus, another possibility for the observed weight change may be due to the oxidation of Al substrate itself. Such measurements were also carried out for ZrO_x/ZrC-ZrN/Zr structures on glass substrate and noticeable weight changes were not present at much higher temperatures, say 400 °C. Considering such degradation limit, ZrO_x/ZrC-ZrN/Zr structures with optimal solar performance $\alpha \sim 0.86$ and $\varepsilon \sim 0.05$ were subjected to the thermal cycling to 150 °C at 5 °C/min heating rate for 2 hours in air ambience to understand the thermal impact on solar performance. The X-ray diffraction patterns were recorded on these thermally treated samples and XRD graphs are plotted in Fig. 4 (a). The observed diffraction planes are in agreement with pristine samples with hexagonal zirconium nitride and zirconium carbide phases in conjunction with zirconium oxide mixed phases. These results suggest the robustness of ZrO_x/ZrC-ZrN/Zr absorber – reflector tandem structures against thermal impact. Surface microstructural degradations were investigated, for these ZrO_x/ZrC-ZrN/Zr heat treated structures, using SEM and AFM measurements and results are summarized in Fig. 4 (b) and (c). SEM micrographs, Fig. 4 (b), did not show any noticeable changes in surface morphology and are consistent with pristine samples, as shown in Fig. 2 (b). AFM measurements also substantiate the SEM results and the observed surface roughnesses are ~ 11.72 nm and ~ 17.85 nm for heat treated ZrO_x/ZrC-ZrN/Zr structures on aluminum and glass substrates. These roughness values are of the same order ~ 10.79 nm and ~ 17.20 nm for pristine ZrO_x/ZrC-ZrN/Zr structures on glass and aluminum substrates, respectively. These observations

suggest that ZrO_x/ZrC-ZrN/Zr structures are highly stable in the investigated temperature range and should have least impact on solar thermal properties.

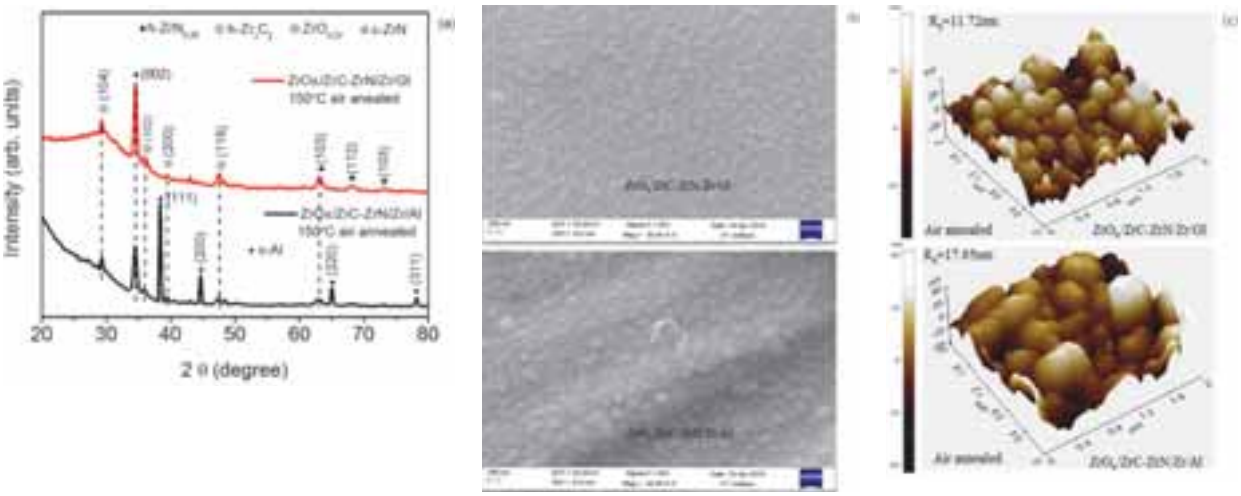

Fig. 4: (a) XRD graphs of air annealed ZrO_x/ZrC-ZrN/Zr absorber-reflector tandem selective structure deposited on glass and aluminum for 2h. **(b) & (c)** SEM and AFM images of air annealed ZrO_x/ZrC-ZrN/Zr absorber-reflector tandem selective structure deposited on glass and aluminum substrates for 2h.

The reflectance measurements were carried out for these ZrO_x/ZrC-ZrN/Zr heat treated samples in the entire 0.2 μm – 25 μm wavelength range and results are summarized in Fig. 5. The measured α and ε values are 0.82 and 0.09 as compared to 0.86 and 0.05 for pristine samples respectively. A small deviation in optical properties of these ZrO_x/ZrC-ZrN/Zr structures may be due to minor surface degradation, not noticeable in the present studies, suggesting insensitivity in the range of investigated temperature. This is in consistent with structural and microstructural measurements, where relatively no substantial changes were observed. These findings suggest that ZrO_x/ZrC-ZrN/Zr may be a good candidate for enhanced solar thermal performance and may exhibit long stability for low and medium temperature applications on glass and aluminum substrates.

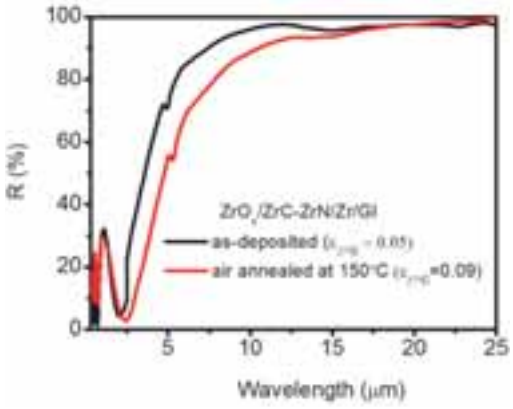

Fig. 5: Reflectance spectra of as-deposited and air annealed ZrO_x/ZrC-ZrN/Zr absorber-reflector tandem selective structure deposited on glass for 2h.

4. Conclusion

ZrO_x/ZrC-ZrN/Zr absorber-reflector tandem structures are optimized for both aluminum and glass substrates for optimal solar thermal performance by tailoring the zirconium nitride content in ZrC-ZrN absorbing layer. The intermediate nitrogen flow rate ~ 10 – 15 sccm has shown the best $\alpha \sim 0.86$ and $\varepsilon \sim 0.05$. The ZrO_x/ZrC-ZrN/Zr structures are stable in air upto ~ 150 °C without any noticeable degradation in their solar thermal performance as compared to pristine samples for both Al and glass substrates.

Acknowledgments

Authors acknowledge Ministry of New & Renewable Energy (MNRE), India through grant 15/40/2010-11/ST for financial support for the work

References

Bogaerts, W. F., and Lampert, C. M.**,** 1983. Materials for photothermal solar energy conversion, J. Mat. Sci. 18, 2847.

Barshilia, H.C., Selvakumar, N., Rajam, K.S., Biswas, A., 2008. Structure and optical properties of pulsed sputter deposited Cr_xO_y/Cr/Cr_2O_3 solar selective coatings, J. of Appl. Phys. 103, 023507(1)-023507(11).

Driver, P. M., 1981. An electrochemical approach to the characterization of black chrome selective surfaces, SEM 4**,** 1799.

Duffie, J.A., Beckman, W.A., 1991. Solar Engineering of Thermal Process, second ed. Wiley Interscience, New York.

Graf, W., Bruker, F., Kohl, M., Troscher, T., Wittwer, V., Herlitze, L., 1997. Development of large area sputtered solar absorber coatings, Journal of Non-Crystalline Solids 218, 380-387.

Holloway, P. H., Shanker, K., Pettit, R. B., and Sowell, R. R., 1980. Oxidation of electrodeposited black chrome selective solar absorber films, SAND-80-1045. Albuquerque, NM: Sandia National Laboratory.

Ignatiev, A., O'Neill, P., and Zajac, G., 1979. The surface microstructure -optical properties relationship in solar absorbers: black chrome, SEM **1,** 69.

Kalogirou, S. A., 2004. Solar Thermal Collectors and Applications, Progress in Energy and Combustion Science, 30, 231-295.

Kennedy, C., 2002. Review of Mid-To High-Temperature Solar Selective Absorber Materilas, NREL/CP-520-31267.

Koltun, M., Gukhman, G., Gavrilina, A., 1994. Stable selective coatings black nickel for solar collector surfaces, Sol. Energy Mater. Sol. Cells 33, 41-44.

Lazarov, M., Sizmann, R., Frei, U., 1993. Optimization of SiO2-TiN_xO_y-Cu interference absorbers, numerical and experimental results, SPIE 2017, 345-356.

Lampert, C. M., 1980, A chemical, structural, and optical characterization of a black chrome solar selective absorber, Ph.D. Thesis, Berkeley, CA: Lawrence Berkeley Laboratory.

McDonald, G. E., 1975. Spectral reflectance properties of black chrome for solar collector use, Sol. Energy, 17**,** 119.

Mekhilef, S., Saidur, R., Safari, A., 2011. A review on solar energy use in industries, Renewable and Sustainable Energy Reviews, 15, 1777-1790.

Selvakumar, N., Barshilia, H. C., 2012. Review of physical vapor deposition (PVD) spectrally selective coatings for mid- and high-temperature solar thermal applications, Sol. Energy Mater. Sol. Cells 98, 1-23.

Seraphin, B.O., 1997. Solar Energy Conversion: Solid State Physics Aspects: Topics in Applied Physics, Vol.31, Springer, Berlin.

Smith, G. B., McPhedran, R. C., and Derrick, G. H., 1985. Surface structure and the optical properties of black chrome, Appl. Phys. A, **36,** 193.

Sweet, J. N., Pettit, R. B., and Chamberlain, M. B., 1984. Optical modeling and aging characteristics of thermally stable black chrome, SEM, **10,** 251.

Sebastian, P.J., Quintana, J., Aliva, F., 1997. Retention of the high optical absorptance in thermally aged black chrome on variably sensitized Cu. Sol. Energy Mater. Sol. Cells 45, 65-74.

Selvakumar, N., Santhoshkumar, S., Basu, S., Biswas, A., Barshilia, H.C., 2013. Spectrally selective CrMoN/CrON tandem absorber for mid-temperature solar thermal applications, Sol. Energy Mater. Sol. Cells 106, 97-103.

Vannoni, C., Battisti, R., Drigo (Eds.), S., 2008. Potential for Solar Heat in Industrial Processes, IEA SHC Task 33 and Solar Paces-Task IV: Solar Heat for industrial Process.

Usmani, B., Vijay, V., Chibber, R., Dixit, A., 2015. Spectrally selective response of ZrO_x/ZrC-ZrN/Zr absorber-reflector tandem structures on stainless steel and copper substrates for high temperature solar thermal application, Sol. Energy, (Accepted)

Wackelgard, E., Hultmark, G., 1998. Industrially sputtered solar absorber surface, Sol. Energy mater. Sol. Cells 54, 165-170.

Zhang, Q.-C., 1998. Stainless-steel-AlN cermet selective surfaces deposited by direct current magnetron sputtering technology, Sol. Energy Mater. Sol. Cells 52, 95-106.

Zhang, Q.-C., Zhao, K., Zhang, B.-C., Wang, L.-F., Shen, Z.-L., Lu, D.-Q., Xie, D.-L., Zhou, Z.-J., Li, B.-F., 1998a. A cylindrical magnetron sputtering system for depositing metal-aluminium nitride cermet solar coatings onto batches of tubes, J. Vac. Sci. Technol. A 16, 628-632.

Zhang, Q.-C., Zhao, K., Zhang, B.-C., Wang, L.-F., Shen, Z.-L., Lu, D.-Q., Xie, D.-L., Zhou, Z.-J., Li, B.-F., 1998b. New cermet solar coatings for solar thermal electricity applications, Sol. Energy 64, 109-114